Case Report

Development of 18F-FLT, 11C-PiB, 18F-THK 5351, and 68Ga-PSMA at the National Cyclotron and PET Centre, Chulabhorn Royal Academy

Chanisa Chotipanich MD[1],
Chetsadaporn Promteangtrong MD[1], Anchisa Kunawudhi MD[1]

[1] National Cyclotron and PET Centre, Chulabhorn Hospital, HRH Princess Chulabhorn College of Medical Science, Chulabhorn Royal Academy, Bangkok, Thailand

Positron emission tomography/computed tomography [PET/CT] is a well-established nuclear medicine hybrid imaging modality with high sensitivity and accuracy afforded by the combination of functional and anatomical information. Up until now, fluorine 18 fluorodeoxyglucose [18F-FDG] has been the workhorse radiopharmaceutical of oncological and neurological PET/CT imaging. However, its main limitation is its nonspecific nature, as the tracer can be taken up by both malignant tumors and inflamed tissues. Newer radiopharmaceuticals are able to retain high sensitivity for cancers with improvements in specificity; this can further improve the accuracy and robustness of PET/CT. In this case series, the authors report on their experiences with 4 cases of 18F-FLT, 3 cases of 11C-PiB, 3 cases of 18F-THK5351, and 3 cases of 68Ga-PSMA PET/CT, highlighting the benefits of these novel non-FDG PET radiopharmaceuticals.

Keywords: PET/CT, Non-FDGPET radiopharmaceuticals, 18F-FLT, 11C-PiB, 18F-THK5351, 68Ga-PSMA

J Med Assoc Thai 2018; 101 [Suppl. 6]: S199-S211
Website: http://www.jmatonline.com

Positron emission tomography/computed tomography [PET/CT] is a well-established nuclear medicine hybrid imaging modality with high sensitivity and accuracy for the diagnosis of diseases, on the basis of the detection of abnormalities in cellular metabolism combined with anatomical imaging. PET/CT has an established role in oncological imaging and emerging roles in the imaging of neurological diseases, with fluorine-18-fluorodeoxyglucose (18F-FDG) being the most widely used radiopharmaceutical. Although 18F-FDG has good sensitivity in the evaluation of a wide array of malignant tumors, the tracer is subject to low specificity, as it can also be taken up by inflammatory tissues. Novel radiopharmaceuticals that are more specific to malignant tumors while retaining a high level of sensitivity have therefore been developed; these should result in overall improvements in diagnostic accuracy.

The National Cyclotron and PET Centre, Chulabhorn Hospital, was established under the vision of Professor Dr. Her Royal Highness Princess Chulabhorn Mahidol, to be the nation's center of excellence in PET imaging, with the aim of promoting research and dissemination of knowledge regarding PET/CT imaging in Thailand. The Centre has strived to abide by Her Royal Highness's intentions, as well as continually exploring and utilizing the most novel radiopharmaceuticals in research and patient care. In this case series, the authors report on experience in using non-FDG PET/CT imaging including 4 cases of 18-FLT, 3 cases of 18F-THK5351, 3 cases of 11C-PiB, and 3 cases of 68Ga-PSMA, to highlight their benefits in diagnostic PET/CT imaging.

Correspondence to:
Chotipanich C, National Cyclotron and PET Centre, HRH Princess Chulabhorn College of Medical Science, Chulabhorn Royal Academy, 54 Kamphaengphet 6, Talat Bangkhen, Laksi, Bangkok 10210, Thailand.
Phone: +66-2-5743355 ext. 1312, **Fax:** +66-2-5744724
E-mail: Chanisa.ja@gmail.com

18F-fluorothymidine (FLT) imaging

18F-FLT is a radiofluorine-labeled thymidine analog used for imaging thymidine kinase I [TK1] activity. Its uptake is known to correlate with cellular proliferation and DNA synthesis during the S-phase of

How to cite this article: Chotipanich C, Promteangtrong C, Kunawudhi A. Development of 18F-FLT, 11C-PiB, 18F-THK 5351, and 68Ga-PSMA at the National Cyclotron and PET Centre, Chulabhorn Royal Academy. J Med Assoc Thai 2018;101;Suppl.6: S199-S211.

the cell cycle[1], and it has now been studied in three main applications: 1) evaluation of treatment response in cancer patients[2], 2) correlations with tumor grade, aggressiveness, and other cellular markers of cell proliferation e.g. Ki-67[3,4], and 3) differentiation of radiation-induced necrosis from recurrent tumor, especially in brain tumors and nasopharyngeal cancers[5,6].

The National cyclotron and PET Centre first produced and used 18F-FLT in March 2017. PET/CT services with this tracer have been used in 4 patients, for the purpose of the differential diagnosis of radiation necrosis from residual/recurrent tumor, as well as for the assessment of brain tumor grade. In all cases, PET/CT with 18F-FLT helped guide or change the management of the patients. The clinical summaries and images from all 4 cases are given below.

Case 1

A 65-year-old man with oligodendroglioma received surgery and radiation within the previous 4 years. Follow-up MRI of the brain revealed interval development of a thick irregular rim-enhancing lesion involving the rostrum of the corpus callosum and the right anterior cingulate gyrus, likely to be progression of the tumor with malignant transformation or radiation necrosis. MRI showed suspicion of low grade diffuse glioma in other brain regions, e.g. the left parietotemporal lobe. PET/CT with F-18 FLT was then performed, and revealed focal increased radiotracer uptake in an ill-defined hypodense lesion at the rostrum of the corpus callosum and the right anterior cingulate gyrus. This had a T/B ratio of 7.76, and was hence suggestive of recurrent high-grade tumor (Figure 1). Other suspicious areas seen on MRI showed no abnormal FLT uptake, implying that they were benign in nature or low-grade tumor. Surgery was performed on the FLT positive mass, and pathology demonstrated glioblastoma multiforme.

Case 2

A 48-year-old man with anaplastic astrocytoma was treated with radiation and Temozolomide. MRI of the brain at 4 months post-treatment revealed a partial treatment response with suspicion of progression that could not be differentiated between radiation necrosis and tumor progression. 18F-FLT PET/CT was therefore performed, and revealed abnormal increased FLT uptake at the right splenium of the corpus callosum and along the periventricular white matter of the atrium, posterior horn, and inferior horn of the right lateral ventricle,

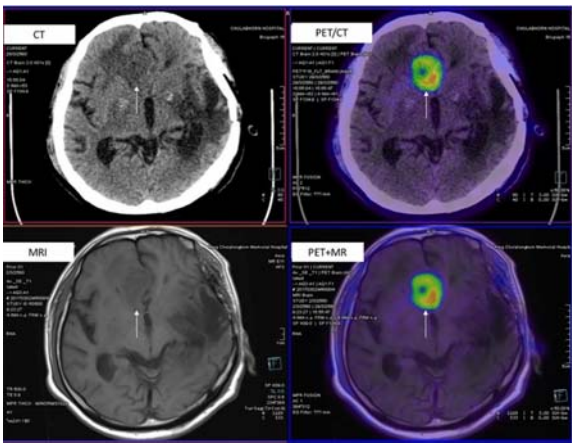

Figure. 1 Abnormal focal increased F-18 FLT uptake of a lesion at the rostrum of the corpus callosum and the right anterior cingulate gyrus (arrow). PET/CT (upper row) and PET fusion with MRI (lower row).

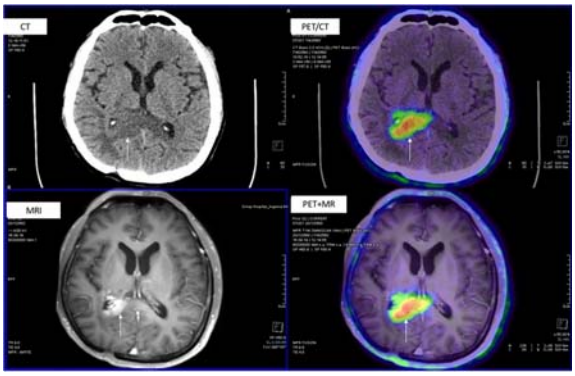

Figure. 2 Abnormal focal increased F-18 FLT uptake of a lesion at the right splenium of the corpus callosum (arrow) on PET/CT (upper row) and PET fusion with MRI (lower row).

which was considered to be likely to represent residual or recurrent tumor (Figure 2). The patient was treated with a new regimen of chemotherapy and improvement of the disease was seen on MRI after the 4th cycle.

Case 3

A 59-year-old man with nasopharyngeal cancer received post-concurrent chemoradiotherapy within the previous 2 years. The patient presented with diplopia and suspicion of bilateral cranial nerve 6 palsy. MRI of the brain and orbits revealed abnormal signal intensities with enhancement of the clivus, petrous apices, and right occipital condyle, which could not be

differentiated between osteoradionecrosis and residual/recurrent tumor. Enhancing soft tissue was also present within the right cavernous sinuses, which was of concern for the presence of residual or recurrent tumor. PET/CT was administered with an 18F-FLT radiotracer and demonstrated abnormal mildly increased radiotracer uptake in the right occipital condyle, with a tumor to background ratio (T/B) of 1.96. It was therefore considered to be suspicious of recurrent tumor (Figure 3). The patient is currently under follow-up.

Case 4

A 32-year-old man presented with ataxia. MRI of the brain revealed an ill-defined mass in the right cerebellar peduncle, involving the cerebellar vermis, right side of the pons, and medulla oblongata, and which was suspicious for glioma and glioblastoma. 18F-FLT PET/CT revealed no abnormal radiotracer uptake by the suspicious lesion, suggesting that it was likely to be benign or a slow-growing tumor (Figure 4). Stereotactic biopsy of the right cerebellar/brain stem lesion demonstrated a subtle increase in glial cells and calcification. The most likely diagnosis was gliosis or low-grade glioma. The patient received Temozolomide treatment and is now under follow-up.

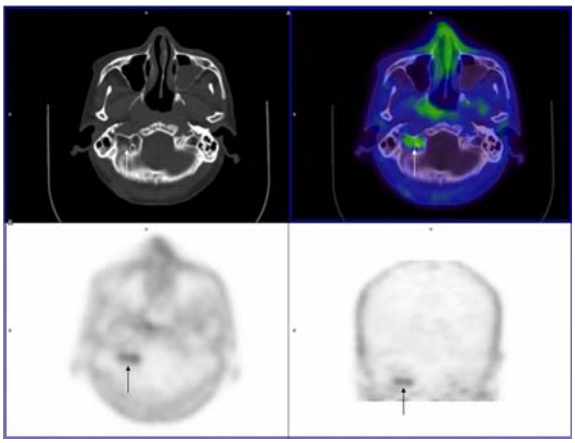

Figure. 3 Increased F-18 FLT uptake at the right occipital condyle (arrow), with a T/B ratio of 1.96.

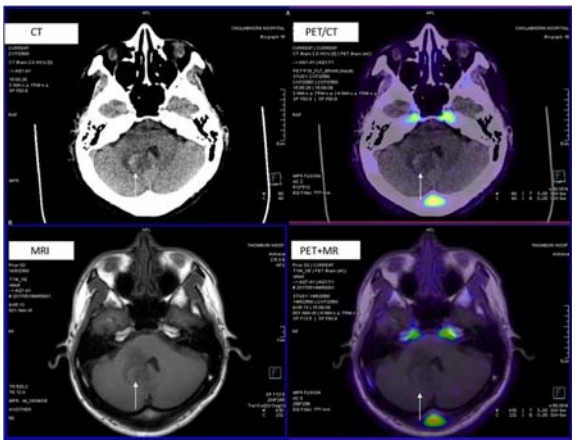

Figure 4 Noabnormal F-18 FLT uptake was observable in a lesion in the right cerebellar peduncle and right lower brain stem (arrow) on PET/CT (upper row) and PET fusion with MRI (lower row).

Discussion

A meta-analysis investigating the diagnostic performance of FLT in the detection of glioma recurrence that included 24 studies[7] revealed a pooled sensitivity of 82% and a specificity of 76%, with the area under the curve [AUROC] of a summary receiver operating characteristic [ROC] curve being 0.85. These findings were slightly better than those of FDG, which showed a sensitivity of 78%, specificity of 77%, and AUROC of 0.84. The performance of FDG was very similar to that found in another meta-analysis, which found values of 77% for both sensitivity and specificity[8]. In short, FLT tends to be more sensitive than FDG, but less specific.

There are heterogeneities in the diagnostic criteria used in FLT PET. Enslow et al[9] studied the use of different parameters from FDG and FLT PET for differentiating recurrent glioma from radiation necrosis and found out that only FDG SUVmax, FDG T/B ratio, and FLT Kimax showed significant differences between the two conditions. FLT Kimax requires kinetic modeling for the analysis, which requires meticulous and attentive work. The visual analysis of FLT showed a sensitivity of 81%, specificity of 50%, and an AUROC of 0.86. In their study of 15 cases, radiation necrosis demonstrated a low uptake of FLT and recurrent glioma showed no uptake of FLT. Nonetheless, a limitation of FLT was reported for non-enhancing brain tumor, with a requirement for break-down of the blood-brain barrier being necessary for tumor uptake[6]. This is not the case for 11C-methionine PET, which can be used without breakdown of the blood-brain barrier, because of a different mechanism of radiotracer incorporation into cells[10].

In this small case series, we used visual analysis and T/B ratio for diagnosis, which may have resulted in a false positive for recurrent tumor in Case No. 1 and a false negative for diagnosis of glioma in

Case No. 4. However, the final conclusions require further follow-up time.

11C-PiB PET imaging

Amyloid-β (Aβ) deposition commonly starts in the preclinical stage of Alzheimer's disease [AD], has increased by the time of AD diagnosis, and remains relatively stable during disease progression. Nonetheless, amyloid imaging could be repeatedly confirmed and could be very suitable for the early diagnosis of AD, by detecting pathological changes before loss in cognitive functioning. Increased cortical PiB retention in individuals with AD in comparison with controls has been described in many studies[11,12]. In the AD groups, the highest tracer binding was detected in prefrontal cortex, precuneus, and posterior cingulategyrus, followed by the lateral parietal cortex, temporal cortex, and striatum. However, amyloid imaging has no role in monitoring disease progression, because the extent of amyloid deposition is not correlated with cognitive impairment. Amyloid PET is suitable for patients with persistent or progressive unexplained mild cognitive impairment [MCI], who satisfy a core clinical presentation as either an atypical clinical course, or an etiologically mixed presentation, as well as those with progressive dementia and an atypically early age of onset. In patients with one of these appropriate criteria, the following characteristics should be present: 1) a cognitive complaint with objectively confirmed impairment; 2) AD as a possible diagnosis in the case of uncertain diagnosis after a comprehensive evaluation by a dementia expert; and 3) the presence or absence of Aβ pathology to increase diagnostic certainty and alter management[13]. In our Centre, we used 11C-labeled radiopharmaceutical Pittsburgh Compound B [PiB] as an amyloid PET tracer. The clinical benefits of 11C-PiB PET in the diagnosis of AD are demonstrated in the following cases.

Case 1

A-64-year-old woman who presented with episodic memory loss. The patient's mini-mental state examination was 5/30. MRI of the brain showed a moderately diffuse brain-volume loss with mild precuneus atrophy. Bilateral hippocampal atrophy was noted (Schelten's score of 3). 11C-PiB PET brain imaging was performed for the confirmation of early onset Alzheimer's disease [EOAD]. Diffuse increased 11C-PiB uptake was noted in the grey matter of neocortical regions, including the frontal lobes, parietal lobes, temporal lobes, and posterior cingulate cortex (Figure 5). The standardized uptake value ratio using the cerebellum as a reference region [SUVr] was 1.58. Abnormal amyloid deposition in the brain confirmed the diagnosis of EOAD.

Case 2

A 63-year-old woman presented with bipolar disorder and psychosis. The patient had episodic memory loss for 1 year. 18F-FDG and 11C-PiB PET scans of the brain were performed for evaluation. Decreased 18F-FDG uptake was noted in the bilateral

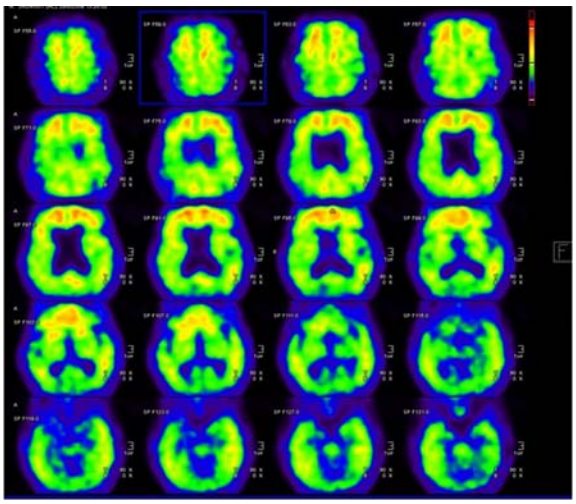

Figure. 5 11C-PiB PET of the brain, axial views with increased tracer uptake visible in the gray matter of the neocortical brain.

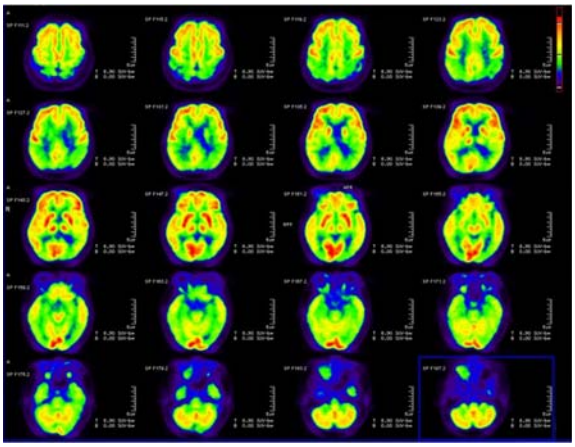

Figure. 6 18F-FDG PET of the brain, axial views with markedly decreased tracer uptake in the bilateral parietotemporal lobes.

parietotemporal lobes, including the precuneus and posterior cingulate cortex (Figure 6). 11C-PiB PET of the brain showed diffuse tracer accumulation in the gray matter of the brain, with an SUVr of 2.12 (Figure 7). The findings suggested AD.

Case 3

A 74-year-old woman presented with episodic memory impairment over 4 years. A Montreal Cognitive Assessment [MoCA] test gave a result of 19/30. The patient had a history of a meningioma in the left frontal lobe, which was removed 5 years previously. MRI of the brain showed brain atrophy in the left frontoparietal cortex and bilateral hippocampus (left hippocampus, Schelten's score 3; right hippocampus, Schelten's score 2). Multiple foci of white matter changes were also noted in the bilateral centrum semiovale and periventricular region (Fazekas scale 2). Differential diagnoses were AD and dementia due to small vessel disease. 18F-FDG and 11C-PiB PET brain scans were performed for confirmation of AD. Decreased 18F-FDG uptake was demonstrated in the bilateral parietotemporal lobes, including the precuneus and posterior cingulate cortex (Figure 8). 11C-PiB PET of the brain showed no abnormal tracer accumulation in the gray matter of the brain parenchyma, with anSUVr of 1.19 (Figure 9). As there was no abnormal amyloid deposition in the brain, the AD process was considered less likely.

Discussion

Cases No. 1 and No. 2 were typical cases of AD presenting with episodic memory loss. In these cases, 11C-PiB PET showed diffuse 11C-PiB retention in neocortical regions and SUVr values of 1.58 and 2.12 respectively. These were suggestive of abnormal amyloid deposition in the brain and confirmed AD pathology. The findings were in concordance with many studies[1,2]. Using post-mortem amyloid burden as a standard, Villeneuve et al[14] reported high sensitivity and specificity of 11C-PiB PET for the detection of abnormal amyloid deposition, with a sensitivity of 83.3% and a specificity of 100% using anSUVr cut off of 1.21.

The clinical presentation of case No. 2 was also episodic memory impairment; however, the 11C-PiB PET imaging of this case showed no abnormal tracer retention in the gray matter of the brain parenchyma using anSUVr of 1.19. Therefore, AD pathology was not evident, and non-AD dementia was diagnosed. A literature review by Zhang et al[15] reported that the sensitivity of 11C-PiB PET for the early detection of

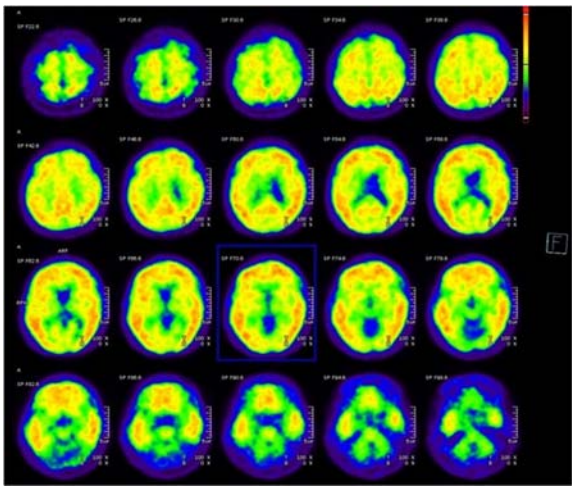

Figure 7 11C-PiB PET of the brain, axial views demonstrating increased tracer uptake in the gray matter of the neocortical brain.

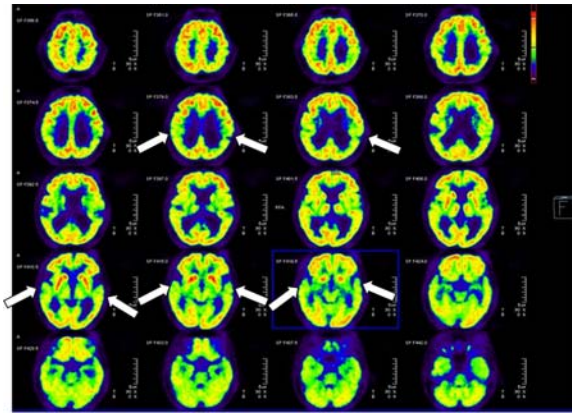

Figure. 8 18F-FDG PET of the brain, axial views showing decreased tracer uptake in the bilateral parietotemporal lobes.

AD was between 83% and 100%, and the specificity was between 46% and 88%, while the positive and negative likelihood ratios were 2.3 and 0.07 respectively. Amyloid imaging would be suitable for ruling out AD in the presence of a PiB negative scan, as a demented patient without Aβ in the brain have AD dementia by definition.

18F-THK 5351 PET imaging

Besides Aβ deposition, the aggregation of tau protein into paired helical filaments and subsequently into neurofibrillary tangles is also a main pathological

process in AD[16]. The deposition of Tau protein in the brain correlates highly with cognitive decline in AD. Typically, tau deposition in AD and MCI due to AD occurs in widespread neocortical regions extending from the temporal lobes towards the parietal cortices and precuneus, with relative sparing of motor regions[17]. Abnormal tau protein deposition is also observed in primary tauopathies, such as progressive supranuclear palsy [PSP], corticobasal degeneration [CBD], and familial frontotemporal dementia. Thus, tau imaging may have clinical benefits for these neurodegenerative diseases[18,19]. High tau PET tracer deposition can be observed in the basal ganglia, thalamus, dentate nucleus of the cerebellum, and midbrain of patients with a clinical diagnosis of PSP[20]. We produce 18F-THK 5351 quinolone derivatives for tau PET imaging, for use in research purposes.

Case 1

A 54-year-old woman known to be diagnosed with EOAD presented with episodic memory loss, dysexecutive syndrome, and behavioral change over 5 years. The MoCA test result was 18/30. MRI of the brain showed no significant hippocampal atrophy (Schelten's score 1, appropriate for the age), but multiple foci of non-specific white matter change in subcortical regions of both the frontal lobes and parietal lobes (Fazekas scale 2). 11C-PiB and 18F-THK 5351 PET imaging of the brain were performed for confirmation of the EOAD diagnosis. Using SUVr cutoff of 1.85, there was increased 11C-PiB uptake in regions of interest including the frontal lobes, parietal lobes, temporal lobes, and posterior cingulate cortices (Figure 10). 18F-THK 5351 PET revealed increased tracer accumulation in areas representative of Alzheimer's disease, including the frontal lobes, parietal lobes, posterior cingulate cortices, precuneus, parahippocampus, fusiform gyrus, and middle and inferior temporal lobes (Figure 11). Abnormal tau and amyloid protein deposition in the brain confirmed the diagnosis of EOAD.

Case 2

A 76-year-old man with a probable case of progressive supranuclear palsy [PSP] presented with downward gaze paresis, frequent falls, dysarthria, depression, and mild dementia. Brain MRI showed marked midbrain atrophy. The patient underwent 18F-FDG, 18F-FDOPA, and 18F-THK 5351 PET imaging of the brain for confirmation of diagnosis. There was no decreased 18F-FDG uptake in the frontal lobe, midbrain,

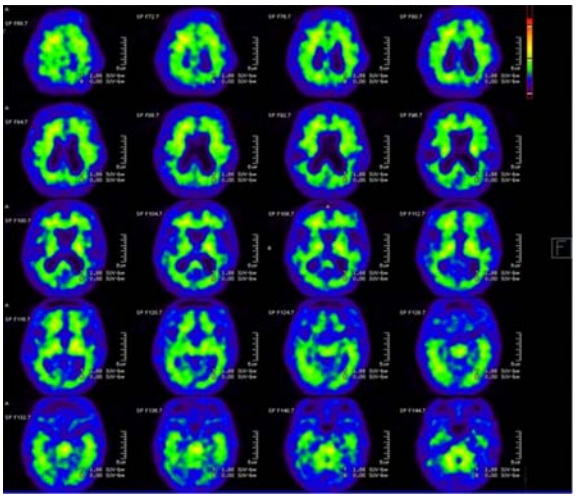

Figure. 9 11C-PiB PET of the brain, axial views showing no tracer uptake in the grey matter of the brain parenchyma,with increased tracer uptake only being noted in the white matter.

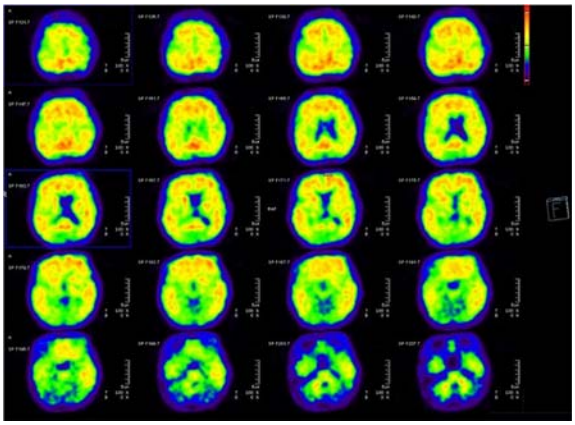

Figure. 10 11C-PiB PET of the brain, axial views showing diffusely increased tracer uptake in the grey matter of the neocortices.

and basal ganglia, which are typical hypometabolic regions in PSP patients (Figure 12). Unremarkable 18F-FDG uptake in the rest of the cortical brain was noted. 18F-FDOPA PET of the brain showed decreased tracer uptake in the bilateral putamen, according to both visual and quantitative analyses (Figure 13). 18F-THK 5351 PET of the brain using standardized uptake value ratio [SUVr] with the cerebellum as a reference region, demonstrated increased 18F-THK 5351 uptake in the inferior temporal cortex, midbrain, and pons in comparison with age-matched cognitively normal Thai

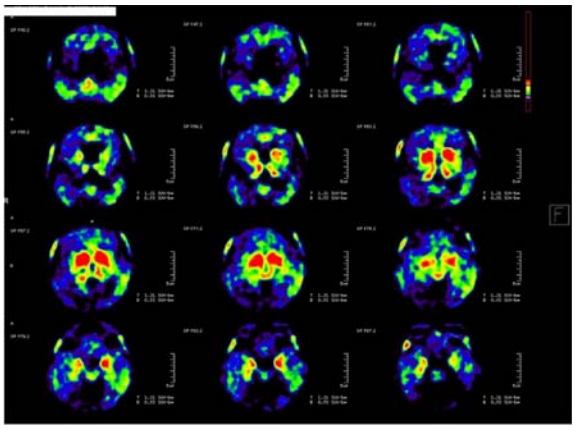

Figure 11. 18F-THK 5351 PET of the brain, coronal views showing abnormal increased tracer uptake in the frontal lobes, parietal lobes, posterior cingulate cortices, precuneus, parahippocampus, fusiform gyrus, and middle and inferior temporal lobes.

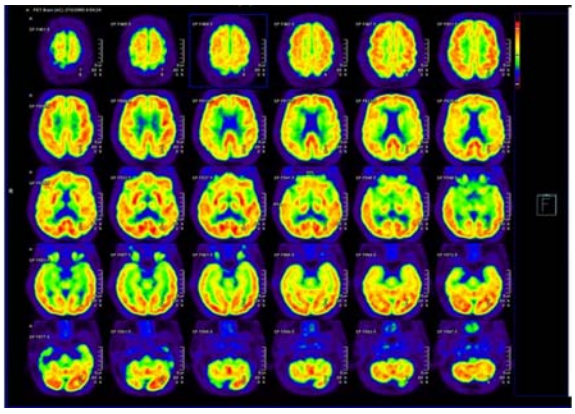

Figure 12. 18F-FDG PET in the brain, axial views with normal tracer uptake and no decrease in tracer uptake in the frontal lobe, midbrain, and basal ganglia, which are typical hypometabolic regions in PSP patients.

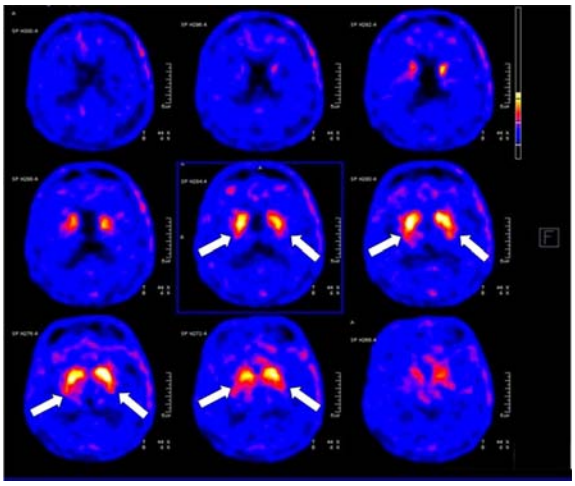

Figure 13. 18F-FDOPA PET of the brain, axial views showing decreased tracer uptake in the bilateral putamen.

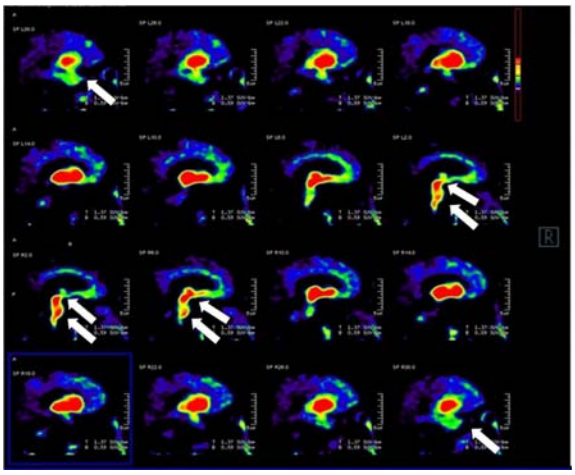

Figure 14. 18F-THK 5351 PET of the brain, sagittal views showing increased 18F-THK 5351 uptake in the inferior temporal cortex, midbrain, and pons.

individuals (Figure 14). No increased 18F-THK 5351 uptake was noted in the caudate, putamen, thalamus, and medulla. According to the literature, abnormal tau deposition in PSP patients is found in the basal ganglia, thalamus, dentate nucleus of the cerebellum, and midbrain. In summary, PET studies of the brain revealed normal 18F-FDG brain uptake but abnormal 18F-FDOPA uptake in the bilateral putamen, with increased tau deposition in areas of the inferior temporal cortex, midbrain, and pons. Parkinson's disease with dementia was given as the probable diagnosis for this patient; however, atypical PSP could not be totally excluded.

Case 3

A 69-year-old woman presented with inappropriate laughter, word finding difficulty, dysexecutive syndrome, and depressed mood for 5 years. PSP and Creutzfeldt-Jakob disease [CJD] were differential diagnoses. MRI of the brain showed right

hippocampal atrophy (Schelten's score 2), moderate bilateral frontoparietal atrophy, and a white matter hyperintensity in the left frontal lobe (Fazekas scale 2). Old multifocal infarctions in the left frontal lobe, right frontal periventricular white matter, left frontoparietal periventricular white matter, and left sided pons were also observed. The patient underwent 18F-FDG, 18F-FDOPA, 11C-PiB, and 18F-THK 5351 PET imaging of the brain for the confirmation of diagnosis. There was decreased 18F-FDG uptake in the left anterior frontal lobe and left parietal lobe, with cross cerebellar diaschisis to the right, compatible with the cerebrovascular disease seen on MRI (Figure 15). Quantitative analysis of 18F-FDOPA PET showed decreased tracer uptake in the bilateral caudate and putamen. Normal amyloid (Figure 16) and tau deposition in areas representative of Alzheimer's disease were noted. However, increased 18F-THK 5351 was observed in the pons in comparison with age-matched cognitively normal Thai individuals (Figure 17). In this case, abnormal tau deposition in the pons with decreased dopaminergic activity in the bilateral caudate and putamen could not exclude atypical PSP.

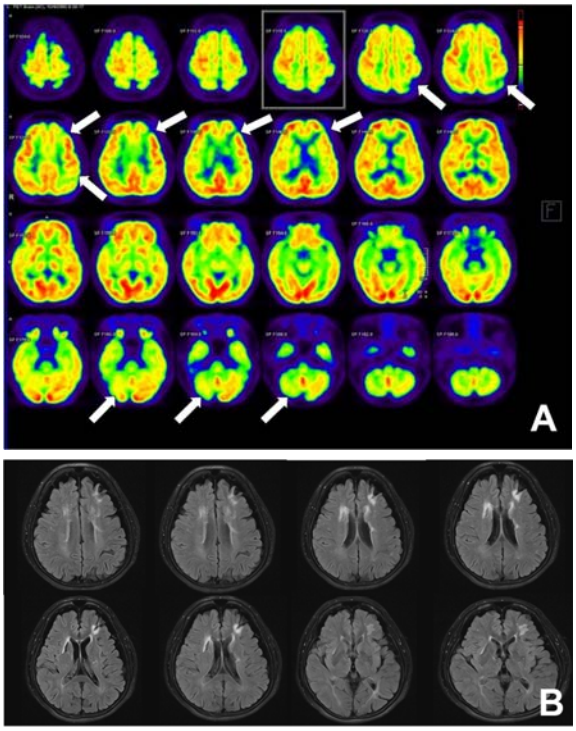

Figure 15. (A) 18F-FDG PET of the brain, axial views showing decreased tracer uptake in the left anterior frontal lobe and left parietal lobe, with cross cerebellar diaschisis to the right, which is compatible with the cerebrovascular disease seen on MRI. (B) MRI brain shows multiple areas of old infarct at left frontal lobe, right frontal periventricularwhite matter, left frontoparietal periventricular white matter.

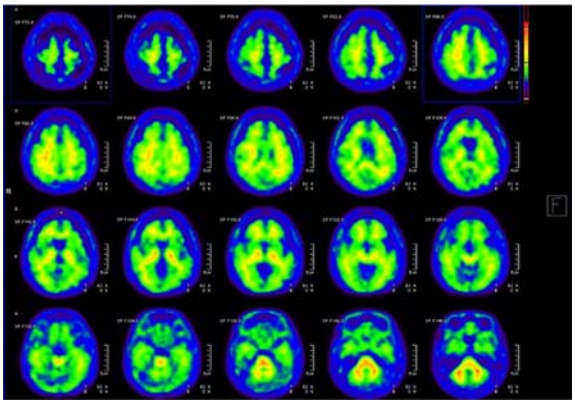

Figure 16. 11C-PiB PET of the brain, axial views showing no abnormal tracer deposition in the neocortices.

Discussion

Case No. 1 underwent tau imaging to confirm a diagnosis of EOAD. The tau imaging of this case showed a typical finding of AD with increased tau tracer uptake in the frontal lobes, parietal lobes, posterior cingulate cortices, precuneus, parahippocampus, fusiform gyrus, and middle and inferior temporal lobes. These findings are in agreement with many studies describing distinct tau tracer retention in AD dementia, amnestic mild cognitive impairment, and normal controls. AD dementia has been reported to show higher tau tracer retention in the frontal, lateral temporal, superior parietal, inferior parietal, anterior cingulate, mesial temporal, hippocampus, entorhinal, fusiform, lingual, and global neocortical areas, with preservation of the primary sensorimotor and primary visual cortices[17,21].

Cases No. 2 and No. 3 were suspected of PSP according to clinical diagnoses and underwent tau imaging for confirmation. In these cases, tau imaging showed findings atypical of PSP. Markedly increased PET tracer uptake indicating tau deposition has been observed in the basal ganglia, thalamus, dentate nucleus of the cerebellum, and midbrain of patients with a clinical diagnosis of PSP[20]. Other studies have reported that clinical PSP patients demonstrate bilaterally elevated tau tracer uptake in the globus

pallidus, putamen, subthalamic nucleus, midbrain, and dentate nucleus relative to controls and PD patients[22]. By contrast, the tau imaging of case No. 2 revealed tracer retention in the inferior temporal cortex, midbrain, and pons, while in case No. 3, a high tau tracer uptake was only seen in the pons. Atypical PSP was the differential diagnosis for these two cases.

68Ga-PSMA

Prostate-specific membrane antigen [PSMA] is a transmembrane protein expressed in prostate gland tissue[23]. PSMA has been found to be elevated in patients with de-differentiated, metastatic, and hormone-refractory prostate cancer[24]. The level of PSMA has also been identified as having prognostic value[25]. Therefore, 68Ga-PSMA PET/CT is a valuable tool for the evaluation of prostate cancer patients with an elevated PSMA level. The first indication for use of this radiopharmaceutical is for localization of tumor tissue in suspected recurrent prostate cancer, where it can help guide salvage therapy[26-28]; 68Ga-PSMA PET/CT is able to detect recurrent disease in patients with PSA levels of 0.2 to 10 ng/ml. The second indication is for primary staging in high-risk disease before surgical procedures or planning of external beam radiation therapy. A growing number of studies have demonstrated that 68Ga-PSMA PET/CT can be superior to CT, MRI, and bone scintigraphy in this respect[29-32]. Other emerging indications for 68Ga-PSMA PET/CT include 1) staging before and during PSMA-directed radiotherapy (mainly in metastatic castration-resistant prostate cancer)[33-36], 2) targeted biopsy after a previous negative biopsy in patients with high suspicion of prostate cancer[37,38], and 3) monitoring of systemic treatment of metastatic prostate cancer. This report now describes three prostate cancer patients who-benefited from 68Ga-PSMA PET/CT.

Case 1

A 75-year-old man with a biochemical recurrence of prostate cancer (PSA 7 ng/ml) was examined in July 2017. Five years previously, the patient underwent radical prostatectomy and received androgen deprivation therapy every 3 months. Recurrent tumor was suspected, and PET/CT was performed with a 68Ga-PSMA radiotracer. This revealed abnormal increased uptake in osteoblastic lesions at the L1 vertebral body and the inferior ramus of the right pubic bone, suggestive of bone metastases (Figure 18).

Case 2

A 67-year-old man with prostate cancer underwent brachytherapy in 2011. In June 2017, the patient presented with an elevated PSA level of 6 ng/mL. Further MRI of the prostate was performed, with findings suspicious of small recurrent prostate cancer [PIRD 4] being found in the right and left medial posterior peripheral zones and left lateral posterior peripheral zone of the midgland, along with left perirectal adenopathy. 68Ga-PSMA PET was performed to confirm the diagnosis and reveal other metastatic lesions, with the result that it showed abnormal increased uptake in a pulmonary nodule in the anterior segment of the RLL, and also in a presacral lymph node, suggestive of pulmonary and lymph node metastases. Additionally,

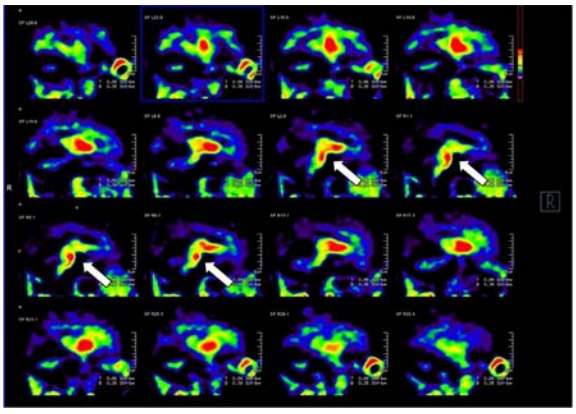

Figure 17. 18F-THK 5351 PET of the brain, sagittal views showing abnormal tracer uptake in the pons.

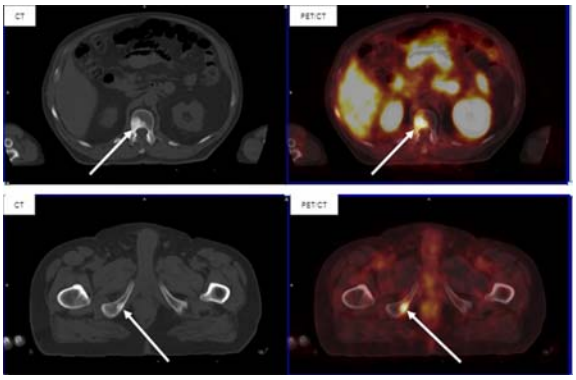

Figure 18. 68Ga-PSMA PET images showing abnormal increased uptake at L1 (upper row) and the right inferior ramus (lower row).

the PET/CT images showed abnormal increased uptake in the prostate, demonstrating malignancy on both sides of the gland (Figure 19).

Case 3

A 75-year-old man with prostate adenocarcinoma underwent radical prostatectomy in March 2017 and post-radiation therapy since July 2017. A serum PSA level of 0.47 ng/mL in August 2017 had increased to 0.915 ng/mL in September 2017. Recurrence of the tumor was then suspected. 68Ga-PSMA PET/CT images revealed a soft-tissue-density lesion with increased uptake abutting the left pelvic side wall (left iliopsoas muscle), a probable metastatic lesion (Figure 20).

Discussion

The three cases presented here demonstrate 68Ga-PSMA PET/CT to be a useful diagnostic modality for detection of local and distant disease foci in patients with biochemical evidence of recurrent prostate cancer. For the detection of bone metastasis in prostate cancer, the sensitivity of bone scanning, CT, and choline PET/CT has been found to be suboptimal. A study by Lengana et al[39] found that 68Ga-PSMA PET/CT had a sensitivity and accuracy of 90.5% and 97.0% respectively for the detection of bone metastasis, which are superior values to those of 73.7% and 86% demonstrated for bone scanning. Hijazi et al[31] reported that 68Ga-PSMA PET/CT yielded a sensitivity, specificity, positive predictive value, and negative predictive value of 94%, 99%, 89%, and 99.5% respectively for the detection of lymph node metastasis from prostate cancer. Vinsensia et al[40] found that 68Ga-PSMA was superior to conventional CT for the detection of lymph node metastasis. 68Ga-PSMA PET/CT has also been shown to be able to detect disease recurrence, even when PSA levels are only minimally elevated. In the cases described in this report, the PSA levels increased from 0.47 ng/mL to 0.915 ng/mL in 2 months, indicating rapidly rising PSA kinetics suggestive of recurrence. In a systematic review and meta-analysis by Von Eyben et al[41], which included 15 articles covering a total of 1,256 patients, 68Ga-PSMA PET/CT was shown to be able to detect recurrent disease after radical prostatectomy, even when PSA levels were <1 ng/mL, with detection of recurrence in 50% of patients with PSA levels of >0.5 ng/mL. 68Ga-PSMA PET/CT is superior to 11C-choline PET/CT for the detection of disease recurrence in patients with PSA <1 ng/mL. For disease staging, the pooled sensitivity and specificity of 68Ga-PSMA PET/CT are

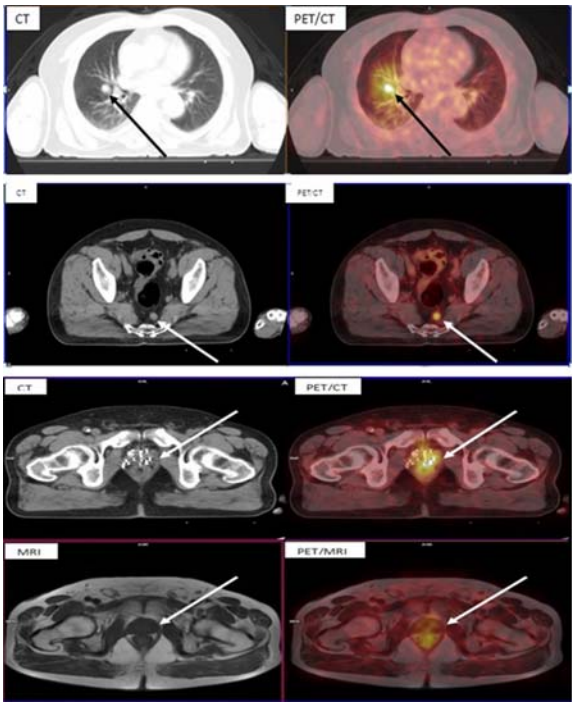

Figure 19. 68Ga-PSMA PET imaging of a hypermetabolic area in a pulmonary nodule located in the anterior segment of the RLL (upper row), and in a presacral lymph node (middle row), as well as uptake in the prostate gland (lower row).

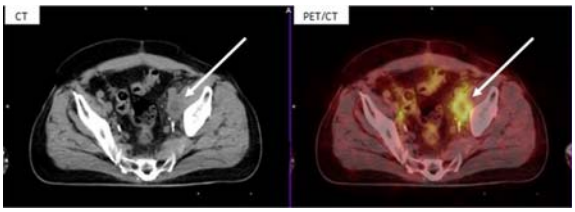

Figure 20. Increased 68Ga-PSMA uptake in a soft-tissue-density lesion abuttingtheleft iliopsoas muscle.

61 to 79% and 84 to 97% respectively. Afag et al[42] reported that 68Ga-PSMA PET/CT could alter management in 39% of prostate cancer patients with evidence of biochemical recurrence [BCR].

Conclusion

From a clinical point of view and based on the majority of published cases, 11C-PiB has strong benefits in the diagnostic evaluation of AD in patients with unclear clinical presentation and those with progressive or persistent unexplained MCI. 18F-

THK5351 can be used for the diagnosis of patients with primary tauopathy, while 18F-FLT performs well in the differentiation of radiation necrosis from residual/recurrent brain tumors, as well as in the assessment of brain tumor grade. Finally, 68Ga-PSMA is a powerful tracer for the diagnostic evaluation of patients with prostate cancer. Thus, production of these PET tracers by the National Cyclotron and PET Centre are very useful and will be very beneficial for patient management.

What is already known on this topic?

PET/CT has a crucial role in oncological imaging and emerging roles in neurological diseases with 18F-FDG as the most widely used radiopharmaceutical. Despite its sensitivity for most malignant tumors, the tracer lacks specificity due to the possibility of inflammatory tissues taken up, thus lowering its specificity. Hence, novel radiopharmaceuticals have been then developed to be more specific to malignant tumors while retaining a high level of sensitivity which would result in the overall improvement of diagnostic accuracy as a potential modality in patient care, and especially in research and knowledge dissemination regarding PET/CT imaging in Thailand.

What this study adds?

The novel non-FDG PET radiopharmaceuticals of 18-FLT, 11C-PiB, 18F-THK5351, and 68Ga-PSMA PET/CT can yield strong benefits in diagnostic PET/CT imaging. 11C-PiB is highlighted in AD with unclear clinical presentation and progressive or persistent unexplained MCI. Meanwhile, 18F-THK5351 is more beneficial in those with primary tauopathy. Whilst, 18-FLT is well established in the differentiation between radiation necrosis and residual/recurrent brain tumors, as well as the assessment of brain tumor grade. In particular, 68Ga-PSMA is potentially powerful in the diagnostic evaluation of prostate cancer cases.

Acknowledgements

We would like to thank Chulabhorn Hospital and Chulabhorn Royal Academy for the funding support towards the success and accomplishment of this study. We sincerely appreciated the University of Tohoku, Sendai, Japan for the provision of the THK precursor throughout the completion of this study. Finally, our gratitude and most appreciation is specially extended to Prof. Eyal Mishani, PhD, Director of Cyclotron/ Radiochemistry unit, Department of Nuclear Medicine, Hadassah Medical Center, Israel, as a visiting professor and a consultant for our radiotracer production at the National Cyclotron and PET Center, Bangkok, Thailand.

Potential conflicts of interest

The authors declare no conflict of interest.

References

1. Herrmann K, Buck AK. Proliferation imaging with (1)(8)F-fluorothymidine PET/computed tomography: physiologic uptake, variants, and pitfalls. PET Clin 2014;9:331-8.
2. Bollineni VR, Kramer GM, Jansma EP, Liu Y, Oyen WJ. A systematic review on [(18)F]FLT-PET uptake as a measure of treatment response in cancer patients. Eur J Cancer 2016;55:81-97.
3. Collet S, Valable S, Constans JM, Lechapt-Zalcman E, Roussel S, Delcroix N, et al. [(18)F]-fluoro-L-thymidine PET and advanced MRI for preoperative grading of gliomas. Neuroimage Clin 2015;8:448-54.
4. Chalkidou A, Landau DB, Odell EW, Cornelius VR, O'Doherty MJ, Marsden PK. Correlation between Ki-67 immunohistochemistry and 18F-fluorothymidine uptake in patients with cancer: A systematic review and meta-analysis. Eur J Cancer 2012;48:3499-513.
5. Chen W, Cloughesy T, Kamdar N, Satyamurthy N, Bergsneider M, Liau L, et al. Imaging proliferation in brain tumors with 18F-FLT PET: comparison with 18F-FDG. J Nucl Med 2005;46:945-52.
6. Shah R, Vattoth S, Jacob R, Manzil FF, O'Malley JP, Borghei P, et al. Radiation necrosis in the brain: imaging features and differentiation from tumor recurrence. Radiographics 2012;32:1343-59.
7. Li Z, Yu Y, Zhang H, Xu G, Chen L. A meta-analysis comparing 18F-FLT PET with 18F-FDG PET for assessment of brain tumor recurrence. Nucl Med Commun 2015;36:695-701.
8. Nihashi T, Dahabreh IJ, Terasawa T. Diagnostic accuracy of PET for recurrent glioma diagnosis: a meta-analysis. AJNR Am J Neuroradiol 2013;34:944-11.
9. Kim SK, Im HJ, Kim W, Kim TS, Hwangbo B, Kim HJ. F-18 fluorodeoxyglucose and F-18 fluorothymidine positron emission tomography/computed tomography imaging in a case of neurosarcoidosis. Clin Nucl Med 2010;35:67-70.
10. Tripathi M, Sharma R, Varshney R, Jaimini A, Jain J, Souza MM, et al. Comparison of F-18 FDG and

C-11 methionine PET/CT for the evaluation of recurrent primary brain tumors. Clin Nucl Med 2012;37:158-63.
11. Klunk WE, Engler H, Nordberg A, Wang Y, Blomqvist G, Holt DP, et al. Imaging brain amyloid in Alzheimer's disease with Pittsburgh Compound-B. Ann Neurol 2004;55:306-19.
12. Rabinovici GD, Furst AJ, O'Neil JP, Racine CA, Mormino EC, Baker SL, et al. 11C-PIB PET imaging in Alzheimer disease and frontotemporal lobar degeneration. Neurology 2007;68:1205-12.
13. Johnson KA, Minoshima S, Bohnen NI, Donohoe KJ, Foster NL, Herscovitch P, et al. Appropriate use criteria for amyloid PET: a report of the Amyloid Imaging Task Force, the Society of Nuclear Medicine and Molecular Imaging, and the Alzheimer's Association. J Nucl Med 2013;54:476-90.
14. Villeneuve S, Rabinovici GD, Cohn-Sheehy BI, Madison C, Ayakta N, Ghosh PM, et al. Existing Pittsburgh Compound-B positron emission tomography thresholds are too high: statistical and pathological evaluation. Brain 2015;138:2020-33.
15. Zhang S, Smailagic N, Hyde C, Noel-Storr AH, Takwoingi Y, McShane R, et al. (11)C-PIB-PET for the early diagnosis of Alzheimer's disease dementia and other dementias in people with mild cognitive impairment (MCI). Cochrane Database Syst Rev 2014;(7):CD010386.
16. Saint-Aubert L, Lemoine L, Chiotis K, Leuzy A, Rodriguez-Vieitez E, Nordberg A. Tau PET imaging: present and future directions. Mol Neurodegener 2017;12:19.
17. Xia C, Makaretz SJ, Caso C, McGinnis S, Gomperts SN, Sepulcre J, et al. Association of in vivo [18F]AV-1451 tau PET imaging results with cortical atrophy and symptoms in typical and atypical Alzheimer disease. JAMA Neurol 2017;74:427-36.
18. Spina S, Schonhaut DR, Boeve BF, Seeley WW, Ossenkoppele R, O'Neil JP, et al. Frontotemporal dementia with the V337M MAPT mutation: Tau-PET and pathology correlations. Neurology 2017;88:758-66.
19. Kikuchi A, Okamura N, Hasegawa T, Harada R, Watanuki S, Funaki Y, et al. In vivo visualization of tau deposits in corticobasal syndrome by 18F-THK5351 PET. Neurology 2016;87:2309-16.
20. Ishiki A, Harada R, Okamura N, Tomita N, Rowe CC, Villemagne VL, et al. Tau imaging with [(18) F]THK-5351 in progressive supranuclear palsy. Eur J Neurol 2017;24:130-6.
21. Kang JM, Lee SY, Seo S, Jeong HJ, Woo SH, Lee H, et al. Tau positron emission tomography using [(18)F]THK5351 and cerebral glucose hypometabolism in Alzheimer's disease. Neurobiol Aging 2017;59:210-9.
22. Schonhaut DR, McMillan CT, Spina S, Dickerson BC, Siderowf A, Devous MD, Sr., et al. (18) F-flortaucipir tau positron emission tomography distinguishes established progressive supranuclear palsy from controls and Parkinson disease: A multicenter study. Ann Neurol 2017;82:622-34.
23. Silver DA, Pellicer I, Fair WR, Heston WD, Cordon-Cardo C. Prostate-specific membrane antigen expression in normal and malignant human tissues. Clin Cancer Res 1997;3:81-5.
24. Ghosh A, Heston WD. Tumor target prostate specific membrane antigen (PSMA) and its regulation in prostate cancer. J Cell Biochem 2004;91:528-39.
25. Ross JS, Sheehan CE, Fisher HA, Kaufman RP Jr, Kaur P, Gray K, et al. Correlation of primary tumor prostate-specific membrane antigen expression with disease recurrence in prostate cancer. Clin Cancer Res 2003;9:6357-62.
26. Afshar-Oromieh A, Hetzheim H, Kratochwil C, Benesova M, Eder M, Neels OC, et al. The theranostic PSMA ligand PSMA-617 in the diagnosis of prostate cancer by pet/ct: Biodistribution in humans, radiation dosimetry, and first evaluation of tumor lesions. J Nucl Med 2015;56:1697-705.
27. Eiber M, Maurer T, Souvatzoglou M, Beer AJ, Ruffani A, Haller B, et al. Evaluation of hybrid (6)(8)Ga-PSMA ligand PET/CT in 248 patients with biochemical recurrence after radical prostatectomy. J Nucl Med 2015;56:668-74.
28. Ceci F, Uprimny C, Nilica B, Geraldo L, Kendler D, Kroiss A, et al. (68)Ga-PSMA PET/CT for restaging recurrent prostate cancer: which factors are associated with PET/CT detection rate? Eur J Nucl Med Mol Imaging 2015;42:1284-94.
29. Maurer T, Gschwend JE, Rauscher I, Souvatzoglou M, Haller B, Weirich G, et al. Diagnostic efficacy of (68)gallium-psma positron emission tomography compared to conventional imaging for lymph node staging of 130 consecutive patients with intermediate to high risk prostate cancer. J Urol 2016;195:1436-43.
30. Herlemann A, Wenter V, Kretschmer A, Thierfelder KM, Bartenstein P, Faber C, et al. (68)Ga-PSMA

positron emission tomography/computed tomography provides accurate staging of lymph node regions prior to lymph node dissection in patients with prostate cancer. Eur Urol 2016;70:553-7.
31. Hijazi S, Meller B, Leitsmann C, Strauss A, Meller J, Ritter CO, et al. Pelvic lymph node dissection for nodal oligometastatic prostate cancer detected by 68Ga-PSMA-positron emission tomography/computerized tomography. Prostate 2015;75:1934-40.
32. Pyka T, Okamoto S, Dahlbender M, Tauber R, Retz M, Heck M, et al. Comparison of bone scintigraphy and (68)Ga-PSMA PET for skeletal staging in prostate cancer. Eur J Nucl Med Mol Imaging 2016;43:2114-21.
33. Rahbar K, Schmidt M, Heinzel A, Eppard E, Bode A, Yordanova A, et al. Response and tolerability of a single dose of 177Lu-PSMA-617 in patients with metastatic castration-resistant prostate cancer: A multicenter retrospective analysis. J Nucl Med 2016;57:1334-8.
34. Baum RP, Kulkarni HR, Schuchardt C, Singh A, Wirtz M, Wiessalla S, et al. 177Lu-labeled prostate-specific membrane antigen radioligand therapy of metastatic castration-resistant prostate cancer: Safety and efficacy. J Nucl Med 2016;57:1006-13.
35. Heck MM, Retz M, D'Alessandria C, Rauscher I, Scheidhauer K, Maurer T, et al. Systemic radioligand therapy with (177)Lu labeled prostate specific membrane antigen ligand for imaging and therapy in patients with metastatic castration resistant prostate cancer. J Urol 2016;196:382-91.
36. Ahmadzadehfar H, Eppard E, Kurpig S, Fimmers R, Yordanova A, Schlenkhoff CD, et al. Therapeutic response and side effects of repeated radioligand therapy with 177Lu-PSMA-DKFZ-617 of castrate-resistant metastatic prostate cancer. Oncotarget 2016;7:12477-88.
37. Eiber M, Weirich G, Holzapfel K, Souvatzoglou M, Haller B, Rauscher I, et al. Simultaneous (68)Ga-PSMA HBED-CC PET/MRI improves the localization of primary prostate cancer. Eur Urol 2016;70:829-36.
38. Giesel FL, Sterzing F, Schlemmer HP, Holland-Letz T, Mier W, Rius M, et al. Intra-individual comparison of (68)Ga-PSMA-11-PET/CT and multi-parametric MR for imaging of primary prostate cancer. Eur J Nucl Med Mol Imaging 2016;43:1400-6.
39. Lengana T, Modiselle M, Lawal I, Boshomane G, Ebenhan T, Vorster M, et al. 68Ga-PSMA-PET/CT and bone scintigraphy imaging for staging of high-risk prostate cancer. J Nucl Med 2017;58(Suppl 1):757.
40. Vinsensia M, Chyoke PL, Hadaschik B, Holland-Letz T, Moltz J, Kopka K, et al. (68)Ga-PSMA PET/CT and volumetric morphology of PET-Positive lymph nodes stratified by tumor differentiation of prostate cancer. J Nucl Med 2017;58:1949-55.
41. Petersen LJ, Nielsen JB, Dettmann K, Fisker RV, Haberkorn U, Stenholt L, et al. (68)Ga-PSMA PET/CT for the detection of bone metastasis in recurrent prostate cancer and a PSA level <2 ng/ml: Two case reports and a literature review. Mol Clin Oncol 2017;7:67-72.
42. Afaq A, Alahmed S, Chen SH, Lengana T, Haroon A, Payne H, et al. 68Ga-PSMA PET/CT impact on prostate cancer management. J Nucl Med 2018;59:89-92.